DOI: 10.26485/0459-6854/2017/67.1/7 PL ISSN 0459-6854

B U L L E T I N

DE LA SOCIÉTÉ DES SCIENCES ET DES LETTRES DE ŁÓDŹ

2017 Vol. LXVII

Recherches sur les déformations no. 1

pp. 91–106

Stanisław Bednarek and Julian Płoszajski

THE MAGNETIC AND ELECTRIC FIELD PRODUCED BY A PROTON BUNCH FROM THE LHC AND PROJECT OF THE CHAMBER FOR INVESTIGATIONS IN THESE FIELDS

Summary

This paper describes the estimation method of the spatial distribution of magnetic field induction and electric field intensity produced by a relativistic beam of charged particles. The described method is applied to estimation of this field distribution in surroundings of proton bunches which are accelerated inside the Large Hadron Collider (LHC). It is demonstrated that such bunches generate pulsed high magnetic fields with induction from a few dozen to a few hundred T within the space of a few cm. The fields are relevant to the successful application of research of materials properties in time intervals in the order of fs, which have not been available until now. We additionally present a design for a special chamber allowing easy introduction of samples into the accelerator, remote measurement and data acquisition.

Keywords and phrases: magnetic field, high pulse, accelerator, particle, beam, application

1. Introduction

Highly pulsed magnetic fields have many important applications in scientific research and modern technology. Generation of these fields is most often achieved by use of coils supplied with high intensity electric current [1–3]. Unfortunately, this method has several deficiencies which limit the upper values of magnetic induction and time duration of these pulses. The most important limitation is the result of the relatively high electric resistivity and limited mechanical strength of coil material as well as its temperature increases. It is for these reasons that during the generation of magnetic fields exceeding magnitudes of 200-300 T, the coil is effectively destroyed. Problems arise additionally from the inductivity of the coil, its connecting conductors and

capacitor banks, all of which limit the pulse rise time. The strongest pulsed magnetic fields with magnitude of 800-1000 T induction are generated using the magnetic flux compression method. Unfortunately, this method does require the application of large quantities of high-explosive materials, which leads to the inevitable destruction of a large part of the experimental device [4, 5].

An original and promising approach to generate high pulsed magnetic fields is the application of particle beams from an accelerator. The first experiments of such type were described by H. C. Siegman and co-researchers [6-8]. The authors of the cited articles focused on revealing the experimental interaction between an electron beam and a magnetized sample. Relativistic electron beams generated by the 50 GeV energy Linear Stanford Accelerator were used in these experiments. The accelerator beam was passed through the sample causing its damage. Therefore, the research method used was a destructive one. Moreover, the cited works provided only an estimated value of the magnetic field induction to which the sample was subjected while the electric field was not taken into account in spite of its apparent presence. Ampere's law, which may be applied to non-relativistic particles only, was used for the purposes of magnetic induction calculations.

In this paper we show a proprietary method of calculating the spatial distribution of the magnetic field induction, which is generated by a relativistic particle beam coming from an accelerator. The method is universal because it uses the Lorentz transformation. Moreover, we additionally calculate the spatial distribution of the electric field intensity. We analyse both fields outside the particle beam, and therefore it is possible to conduct non-destructive research. The developed method has been applied to calculations of fields, which are generated by the proton beam accelerated in the LHC. In the final part of the article we have described the design for a special chamber which may be installed next to the accelerator beam tube. The chamber allows for the remote controlled exchange of the examined samples as well as the transfer of the measurement results. Construction of such a chamber would facilitate wide applications of accelerator particle beams in materials research. The proposed method would permit the use of high and ultra-short pulsed magnetic fields, in up to now unprecedented time intervals.

2. Calculation method

At the beginning we estimated the spatial field distribution within the coordinate system connected with a charged particle bunch in motion. Only an electric field exists within this coordinate system because the particles are not moving with regard to the system. The particle beam consists of separated bunches which have an axial symmetry. For purposes of calculations we assumed a rectangular $0xy$ coordinate system moving together with the bunch. Because of the bunch's axial symmetry, we may initially analyse the distribution in two dimensions. We assign the $0x$ axis of the coordinate system to be parallel to the bunch axis and direction of movement, Fig. 1.

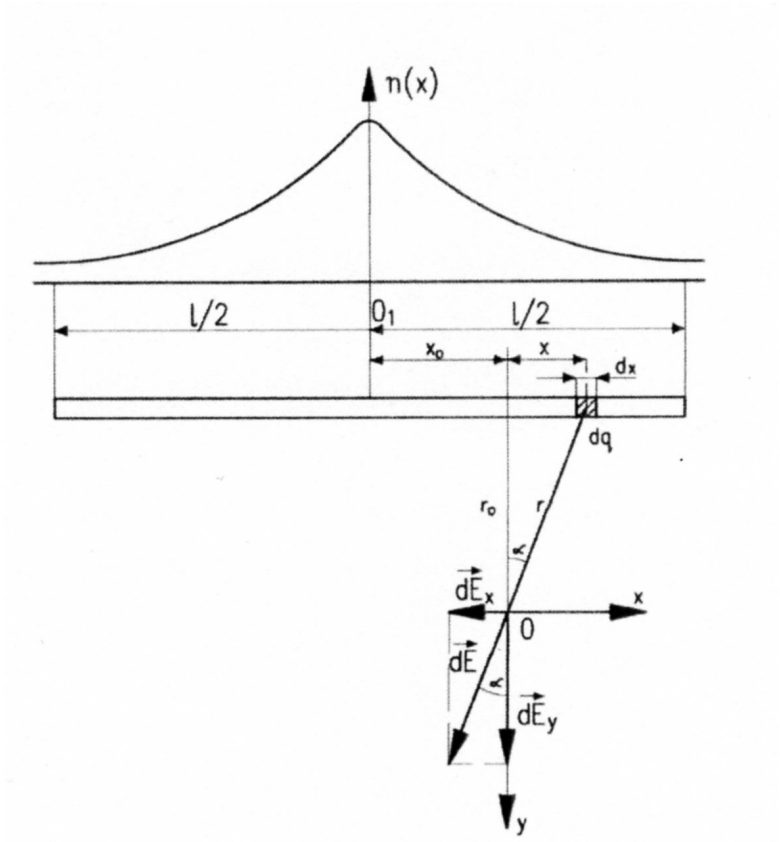

Fig. 1: Frame of reference connected with the particle bunch accepted for calculations; 0_1 – the centre of the bunch, 0 – the point chosen for calculations of the field intensity, $n(x)$ – linear particles density, $l/2$ – half length of the bunch, dq – the charge element, dE_x, dE_y, dE – elements of electric field intensity respectively: longitudinal, transversal and the resultant, r_0 – the distance of the point of calculations from the beam (also bunch) axis, x_0 – translation of the calculation point due to the centre of the bunch calculated in the bunch frame of reference.

Axis $0y$ will then have a radial direction and one which is perpendicular to the direction of the movement. Each bunch has a length of l while the charge density in the bunch is described by the Gauss distribution as having a maximum in the centre [9–11]. The transversal dimensions of the bunch are measured in tens of μm. The examined sample will be placed at a distance of r_0 from the bunch axis amounting to several mm. It means that transversal dimensions of the bunch are considerably less than r_0. We may in this situation omit the change of charge density in the radial direction and assume for the calculations a one-dimensional normal distribution. The linear charge density $\rho(x_1)$ is for this distribution a function of the distance $x_1 =$

$x + x_0$ from the centre of the bunch 0_1 and is expressed by the formula:

$$\rho(x_1) = \frac{n_1 e}{\sigma_x \sqrt{2\pi}} \exp[-\frac{(x+x_0)^2}{2\sigma_x^2}], \tag{1}$$

where: n_1 represents the number of all charges within the bunch, σ_x is the standard deviation for a normal distribution while the symbol e represents an elementary charge.

As mentioned earlier, the coordinate system connected with the bunch includes only an electrical field. The element of the electric field vector dE, generated by the charge element of the bunch $dq = \rho(x_1) \cdot dx$ at the point 0, which is at the distance r from the centre of the element, is expressed by the well-known in electrostatics formula [12].

$$dE = \frac{1}{4\pi\varepsilon_0} \frac{dq}{r_0^2 + x^2}. \tag{2}$$

Field components dE_x, dE_y, are respectively directed along the $0x$ and $0y$ axes and are expressed by the formulas:

$$dE_x = dE \cos\alpha = dE \frac{r_0}{\sqrt{r_0^2 + x^2}}, \tag{3}$$

$$dE_y = dE \sin\alpha = dE \frac{x}{\sqrt{r_0^2 + x^2}}. \tag{4}$$

After substitution of both formulas (1) and (2) respectively into formulas (3) and (4), the following formulas for calculated components dE_x, dE_y at point 0 are obtained:

$$dE_x = \frac{n_1 e}{4\pi\sqrt{2\pi}\varepsilon_0\sigma_x} \frac{x \exp^{-[\frac{(x+x_0)^2}{2\sigma_x^2}]}}{(r_0^2 + x^2)^{3/2}} dx, \tag{5}$$

$$dE_y = \frac{n_1 r_0 e}{4\pi\sqrt{2\pi}\varepsilon_0\sigma_x} \frac{\exp^{-[\frac{(x+x_0)^2}{2\sigma_x^2}]}}{(r_0^2 + x^2)^{3/2}} dx. \tag{6}$$

The complete components of the electrical field intensity E_x, E_y at point 0 are calculated by integrating expressions (5) and (6) after the entire length l of the given bunch. These integrals are expressed by means of the following formulas:

$$E_x = \frac{n_1 e}{4\pi\sqrt{2\pi}\varepsilon_0\sigma_x} \int_{-(\frac{l}{2}+x_0)}^{(\frac{l}{2}-x_0)} \frac{x \exp^{-[\frac{(x+x_0)^2}{2\sigma_x^2}]}}{(r_0^2 + x^2)^{3/2}} dx, \tag{7}$$

$$E_y = \frac{n_1 e r_0}{4\pi\sqrt{2\pi}\varepsilon_0\sigma_x} \int_{-(\frac{l}{2}+x_0)}^{(\frac{l}{2}-x_0)} \frac{\exp^{-[\frac{(x+x_0)^2}{2\sigma_x^2}]}}{(r_0^2 + x^2)^{3/2}} dx. \tag{8}$$

Further we designate the spatial distribution of the magnetic and electric fields within the coordinate system $0x'y'z'$ with the analysed sample at rest. The axes of this system are directed in parallel to the appropriate axes of the previously

accepted $0xy$ system, which is associated with the bunch. It is for this purpose that the Lorentz transformation should be applied to the calculated E_x, E_y components. This transformation is expressed by means of the following general formulas [13]:

$$E_x^{'} = E_x \qquad E_y^{'} = \gamma(E_y - vB_z) \qquad E_z^{'} = \gamma(E_z + vB_y), \tag{9}$$

$$B_x^{'} = B_x \qquad B_y^{'} = \gamma(B_y + \frac{\beta}{c}E_z) \qquad B_z^{'} = \gamma(B_z - \frac{\beta}{c}E_y). \tag{10}$$

All quantities as part of the formulas bearing the „prim" designation refer to the system associated with the sample. In accordance with this B'_x, B'_y, B'_z indicate the components of the magnetic field induction vector within the sample's system while B_x, B_y, B_z represent the magnetic field induction vector components within the reference system of the bunch. Symbols c, β and γ represent respectively: speed of light in a vacuum, ratio of the particle velocity v to the speed of light in a vacuum ($\beta = v/c$) as well as so-called Lorentz factor as expressed by the formula

$$\gamma = \frac{1}{\sqrt{1-\beta^2}}. \tag{11}$$

In accordance with earlier obtained results, the reference system of the bunch includes only two electric field components $E_x, E_y \neq 0$. Therefore, after the application of the Lorentz transformation we obtain as a result of the formulas (9), (10) the following:

$$E_x^{'} = E_x \qquad E_y^{'} = \gamma E_y \qquad E_z^{'} = 0, \tag{12}$$

$$B_x^{'} = 0 \qquad B_y^{'} = 0 \qquad B_z^{'} = -\gamma\frac{\beta}{c}E_y. \tag{13}$$

Formulas (7), (8) as well as (12) and (13) have been used for calculating the electric field intensity components as well as the magnetic induction within the sample reference system. For simplification purposes, the B'_z magnetic field induction component will be referred to henceforth in this article as B.

3. Calculations results

For calculations were used data which are collected in Table 1 that was elaborated on the ground of parameters available in literature, describing the proton beam in the LHC [14]. Moreover, the standard deviation of the Gauss distribution $\sigma_x = 0.2690 \cdot (l/2)$ was accepted. It means that outside of an "l" long section the linear charge density is less than 0.1% of the maximum density in the middle of the bunch and it is the value, which we may omit. The spatial distributions of the components of E'_y, E'_x electric field intensity are shown in Figs. 2, 3.

The spatial distribution of B magnetic field induction was shown in Fig. 4.

For better estimation of usefulness of those fields for research, in Figs. 5–7 were given dependencies of components of E'_x, E'_y electric field intensity B and magnetic

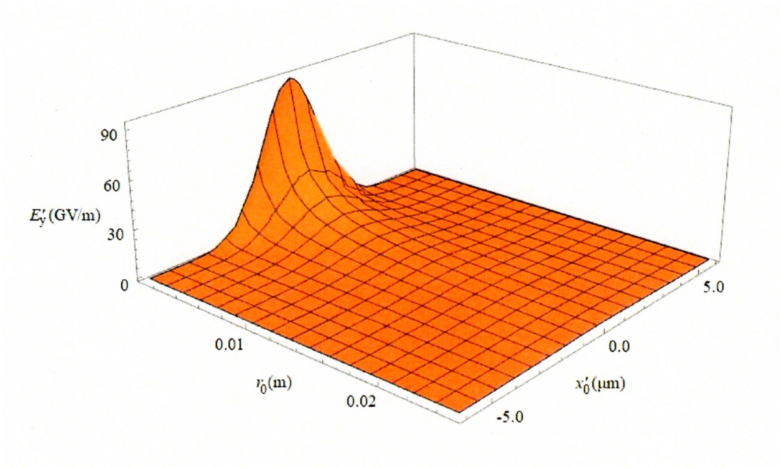

Fig. 2: Spatial distribution of transversal component of the E'_y electric field intensity in the sample frame of reference; r_0 – the distance of the point of calculations from the beam axis, x'_0 – translation of the calculation point due to the centre of the bunch calculated in the sample frame of reference ($x'_0 = x_0/\gamma$).

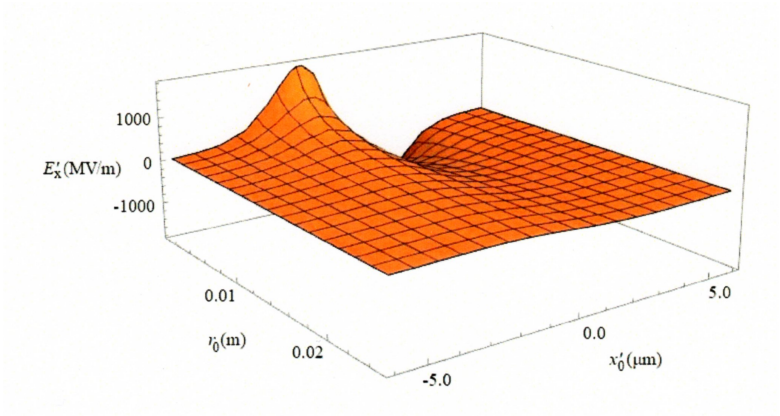

Fig. 3: Spatial distribution of the longitudinal component of the E'_x electric field intensity in the sample frame of reference; coordinates r_0, x'_0 have the same meaning, like in Fig. 2.

field induction, as a function of the r_0 distance from the bunch axis. The r_0 distance is measured in the transversal plane of the bunch symmetry, perpendicular to its movement direction. In this plane $x_0 = 0$.

At the next Figs. 8–10 dependencies of the components from Figs. 5–7 were shown as functions of x_0 distance from mentioned transversal plane of symmetry for fixed r_0 distance = 0.005 m (5 mm) from the bunch axis. The charts in Figs. 5–10 are cross-sections received from Figs. 2–4. The choice of the distance $r_0 = 0,5$ mm from

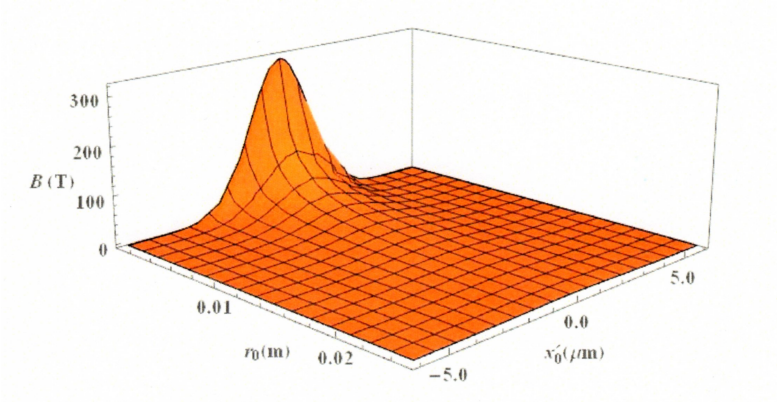

Fig. 4: Spatial distribution of B magnetic field induction in the sample frame of reference; coordinates r_0, x_0' have the same meaning, like in Fig. 2.

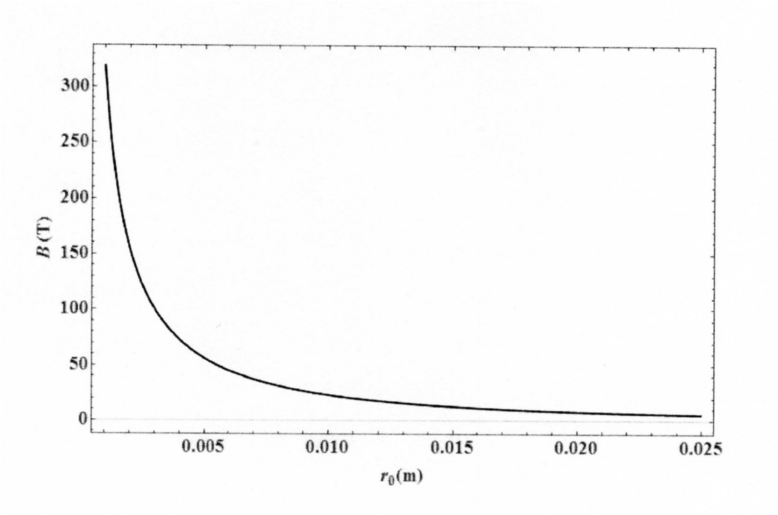

Fig. 5: Dependence of the B magnetic field induction, as a function of the distance from the bunch axis r_0 in the transversal plane of the bunch symmetry ($x_0' = 0$) in the sample frame of reference.

the bunch axis is motivated by the practical attitude because it is possible to place an examined sample, approximately 1 mm in size, at this particular distance.

4. Discussion of results

The obtained results show that the maximal values of the B magnetic field induction are at the transversal plane of symmetry of the bunch for which $x_0 = 0$ (Figs. 4,

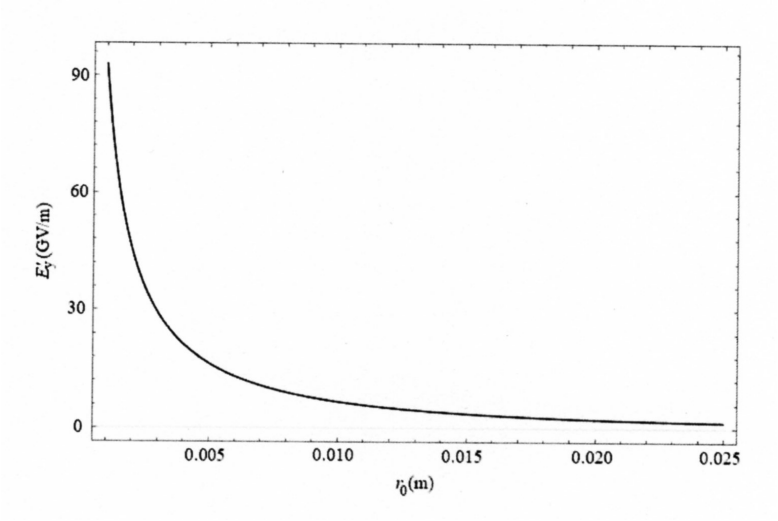

Fig. 6: Dependence of the E'_y component of electric field intensity, as a function of distance from the bunch axis r_0 in the transversal plane symmetry ($x'_0 = 0$) in the sample frame of reference.

5). The maximal values appear at the moment when the centre of the bunch passes in minimal distance from the sample. The proton bunch diameter is approximately 32 μm (Tab. 1).

Tab. 1: Parameters of the proton beam in the LHC

No.	Name of parameter	Symbol	Value
1.	Number of particles (protons) in the bunch	n_1	$1,15 \cdot 10^{11}$
2.	Bunch length	l	7,55 cm
3.	Bunch radius	r_p	16 μm
4.	Particles' energy	E	7 TeV
5.	Particle speed	v	$0,999999991c$
6.	Energy increase (Lorentz factor)	γ	$7,46 \cdot 10^3$
7.	Number of bunches in the pipe	N	2808
8.	Length of tube perimeter	L	25,55 km

We assume that dimensions of examined samples will be approximately 1 mm and such samples are going to be placed at the distance of $r_0 = 1$ mm or larger from the bunch axis. For accepted assumption we see in Fig. 7 that the upper limit of the magnetic field induction helpful in research of the samples at millimetre scale is about 160 T. This value decreases with the distance from the bunch axis. As shown in Fig. 7, at the distance $r_0 = 5$ mm from the bunch axis the value is equal to 60

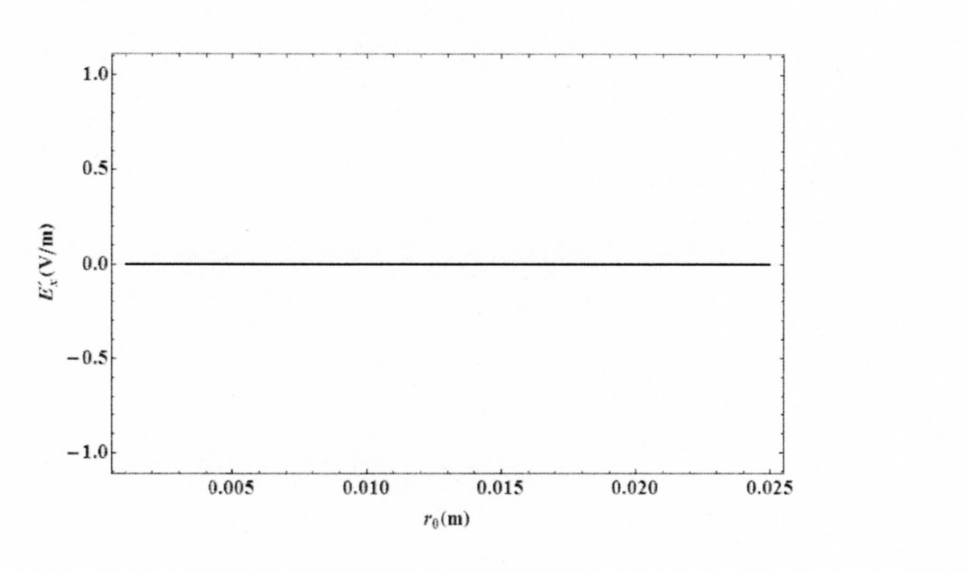

Fig. 7: Dependence of E'_x electric field component intensity, as a function of distance from the bunch axis r_0 in the transversal plane of the bunch symmetry ($x'_0 = 0$) in the sample frame of reference. B magnetic field induction, as a function of the distance x'_0 from the transversal plane of the bunch symmetry for a fixed distance from the bunch axis $r_0 = 0.005$ m in the sample frame of reference.

T. Those magnetic induction values are comparable to field inductions generated by the coils [1, 2]. For comparison, we inform that at the distance $r_0 = 50$ mm from the bunch axis (the distance equal to the radius of the accelerator tube) magnetic field induction decreases to 6 T.

If the sample is placed further from the bunch axis then the maximal field induction value will be less but more homogenous. For the purpose of better quantitative estimation of magnetic field inhomogeneity we consider a cubic sample with a side length of 1 mm. Let the centre of the sample be r_0 at the distance from the bunch axis and its side be parallel to r_0 direction. Magnetic field inhomogeneity at the sample area will be defined by the formula

$$k = \frac{|B_k - B_0|}{B_0} 100\%, \tag{14}$$

where B_k, B_0 mean the magnetic field induction respectively: at the centre and at the edge of the sample. For the mentioned value of $r_0 = 5$ mm, the magnetic field induction at the sample centre is $B_0 = 60$ T but for a distance of $r_0 = 10$ mm the induction at the centre of the sample decreases to $B_0 = 35$ T. It is easy to calculate, using formula (14) and Fig. 5, that in the first case $k < 9\%$ but in the second case $k < 7\%$.

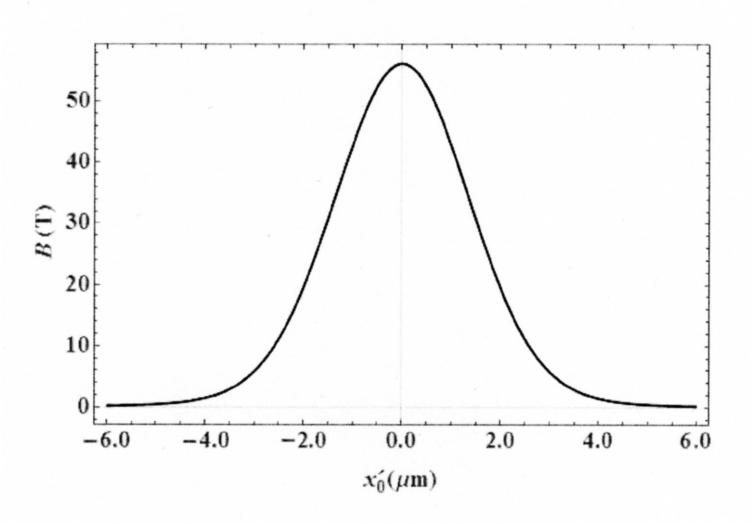

Fig. 8: Dependence of the B magnetic field induction, as a function of the distance x'_0 from the transversal plane of the bunch symmetry for a fixed distance from the bunch axis $r_0 = 0.005$ m in the sample frame of reference.

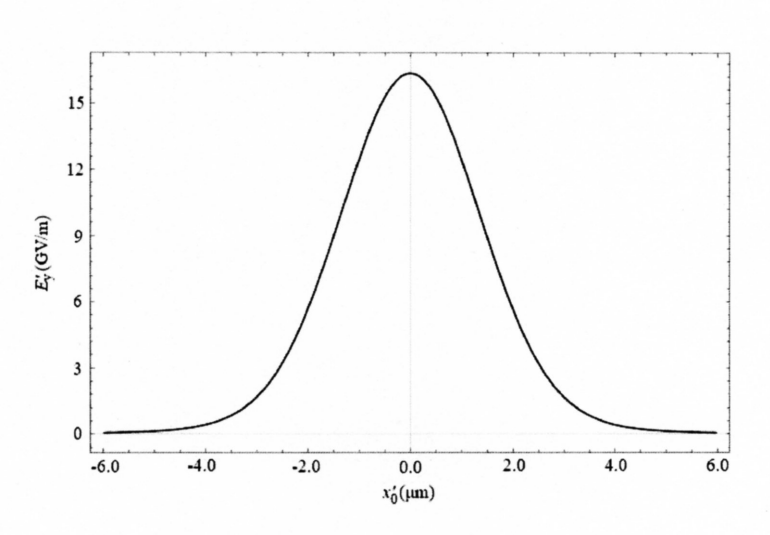

Fig. 9: Dependence of the E'_y component of the electric field intensity, as a function of the distance x'_0 from the transversal plane of the bunch symmetry for fixed distance from the bunch axis $r_0 = 0.005$ m in the sample frame of reference.

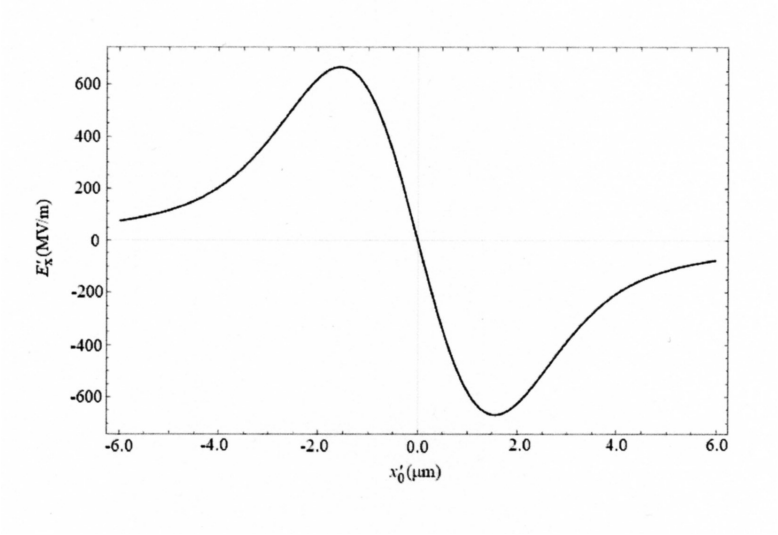

Fig. 10: Dependence of the component of the E'_x electric field intensity, as a function of the distance x'_0 from the transversal plane of the bunch symmetry for fixed distance from the bunch axis $r_0 = 0.005$ m in the sample frame of reference.

We encounter a comparable magnetic field inhomogeneity in the sample in the case of magnetic fields generated by coils. Therefore, this inhomogeneity is not a distinctive feature of fields generated by the particle bunch and it is not a fundamental obstacle in conducting such a research. The radius of the tube in which the bunch moves is 5 cm and it is for this a reason that maximal volume of the sample could be no more than a few cm^3 [14]. Because of the magnetic field inhomogeneity in such a large sample, its optimal volume should be limited to tens of mm^3. It is not a serious limitation too, because we know of cases of research in high magnetic fields samples even of several $\mu\mathrm{m}^3$ [15]. The research of small-sized samples is consistent with a current need of miniaturization in electronics and nanotechnology.

A sample placed nearly to the bunch will also be subjected to the effect of an electric field pulse with E'_x, E'_y components (Figs. 2, 3, 6, 7 and 9, 10). The E'_x component has a maximum and minimum which are equal in value and have opposite signs (Fig. 3). Moreover, $E'_x = 0$ at the plane of the bunch symmetry (Fig. 6). Therefore, we may say that E'_x is an antisymmetric function of x_0. The spatial distribution of the E'_y component is similar to the spatial distribution of the B magnetic field induction due to the Lorentz transformation (see formula 13) where B and E'_y values are directly proportional. An action of the electric field pulse on a sample appears also in the case of magnetic field pulses generated in the usual way with coils or magnetic flux compression. We observe the electric field because, in accordance with Faraday's induction law, variable magnetic field generates the variable electric field.

Screens made of conducting materials provides a simple protection from such a field. Such protection of the measuring devices and samples is practiced in the case of pulsed magnetic fields which are generated in conventional ways. The difference is that the conductor with a current (coil) is electrically neutral and does not generate an electric field but a moving particle bunch does generate one. Hence, the electric field does not constitute any obstacle in research.

Particle bunches have a velocity very close to the speed of light. Therefore, we call them ultra-relativistic particles. It is for this reason that we may not use Ampere's law for calculations of the magnetic field induction generated by the particles. This law may be applied to the calculations of the magnetic field which is generated by the particles moving with small velocities in comparison with the speed of light in a vacuum ($v \ll c$). Then, according to the (11) formula the Lorentz factor $\gamma \approx 1$ and the last formula (13) after the conversions gives a "classic" formula which is applied in technical calculations for magnetic field induction around a straight wire with a current. From (12) and (13) formulas it follows that failure in taking into account the factor γ yields lower values for B magnetic field induction and E'_y electric field intensity in the sample frame of reference. Moreover, for relativistic particles a Lorentz contraction occurs for the spatial distribution of electric field, which is observed in the sample frame of reference. The distribution takes shape of disc, which is very flattened in the direction of particle bunch movement. The Lorentz contraction of the bunch makes it possible to generate unusually short magnetic field pulses which last approximately 4 fs.

5. Project of a chamber

Interior of the accelerator tube is a high vacuum environment with very significant volume while its exterior is subject to atmospheric air pressure. Direct introduction of an examined sample into the tube could be very inconvenient due to the loss of a vacuum and subsequent need for the tube to be purged of air. It would be a time-consuming and labour-intensive procedure. Moreover, during operation of the accelerator, synchrotron radiation is generated which in turn causes material activation within direct surroundings of the tube. As the result, secondary radiation is additionally emitted also after the beam is switched off. To decrease the intensity of this radiation to a secure level, it is necessary to wait for an appropriately long time. Entering the accelerator tunnel during this time is either impossible or requires special protection.

In order to eliminate the described complications, a special chamber for the remote control of exchanging of samples has been designed. A diagram of such a chamber is illustrated in Fig. 11.

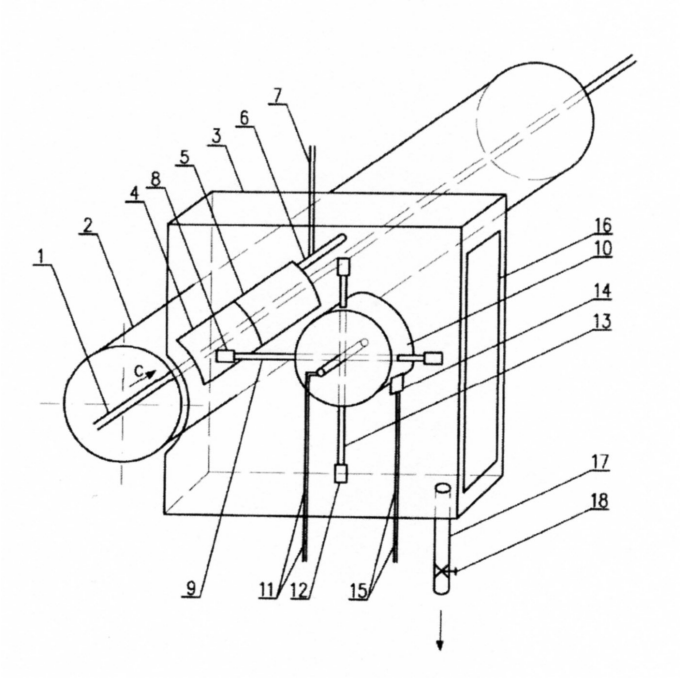

Fig. 11: Scheme of the chamber for remote control exchange of the samples; 1 – particle beam, 2 – accelerator tube, 3 – sample chamber, 4 – window, 5 – inner cover, 6 – propulsion of the inner cover, 7 – connectors supplying cover propulsion, 8 – examined sample, 9 – the examined sample arm, 10 – rotary head with stepper motor, 11 – wires powering the stepper motor, 12 – sample waiting for an exam, 13 – arm of the waiting sample, 14 – switches for collecting measured signals, 15 – wiring connecting the measured signals, 16 – outer cover, 17 – pipe connecting the chamber with the vacuum pump, 18 – valve.

The chamber (3) is located directly adjacent to the accelerator tube (2). From the side accelerator tube, the chamber has a well-sealed inside cover (5), which is remotely controlled by a motor (6). The cover can open or close the window (4) in the accelerator tube (2). The chamber contains a rotary head (10), driven by a remote controlled stepper motor. The head is equipped with several radially distributed arms (9, 13). Samples (8, 12) are located at the end of each arm. One of the samples (8) is being examined at the moment while the rest of the samples is awaiting testing. The surface of the head includes switches which are contacted by fixed brushes (14). The switches are connected to wires (15), leading to the samples. Conductors and brushes are assigned to collect signals produced during the examination such as the magneto-resistivity. Moreover, the chamber is equipped with a hermetic outer cover (16), located opposite the rotary head, and pipe (17) with the valve (18) which is connected to a vacuum pump.

The principle of the chamber's operation is fairly uncomplicated. The outer cover (16) is open during the accelerator's off-time. It is possible at such time to place samples designated for examination on the arms of the rotary head (10). The inner cover (5) is closed then and the accelerator pipe is again brought into a state of vacuum. When the samples are placed, the outer cover is closed. Next, the chamber is purged of air to establish a vacuum as inside the accelerator tube and valve (18) is closed. After the accelerator begins operating, the inner cover (5) is moved and window (4) is opened. The sample (8) located on the turning head (10) is entered into the accelerator tube (2) through the window (4). Opening the cover and the head rotation are remotely controlled. The length of the arm (9) makes it possible to place the chosen sample (8) at the required distance from the bunch axis. (In a more advanced model of the chamber design, this distance can be varied by remote control during the measurements using, for example, telescopic arms.) After finishing the examination of the chosen sample, the head (10) is turned in order to introduce the next sample into the accelerator tube. After completion of all the sample tests, the inner cover (5) is opened and the air pressure is increased to match the ambient pressure. At this time, the chamber is ready for the opening of the outer cover (16) and exchanging of all samples.

6. Conclusions

An application of the accelerator beam for generation of high, pulsed magnetic fields eliminates many problems relevant to coil warming, tensions and damage. Using the non-destructive method makes it possible to obtain repeatable pulsed magnetic fields. A crucial advantage of using the particle beam is the low cost involved. In the case of research using this method, it is not necessary to bear costs connected with the building of the field source because the accelerator already exists for other purposes. The research into the magnetic field generated by the beam from an accelerator could be a new "added value" for this device. It is not necessary to pay for electrical energy because it is an element of regular accelerator activity operating costs. It is worthwhile to consider the possibility of installing the suggested experimental chamber during the construction of newly-designed accelerators or during modernization or maintenance down-time of existing accelerators. Because magnetic fields generated by particle bunches from accelerators have unique parameters unachievable by other methods, they open up a new field of exploration and we may expect significant discoveries as its direct result. They allow us to research very quick processes of remagnetisation. An application of those processes could allow development of magnetic materials useful in building data storage discs with very rapid recording times as well as very quick access to the stored data.

References

[1] H. Ding, Y. Yuan, Y. Xu, C. Jiang, L. Li, X. Duan, Y. Pan, J. Hu, *Testing and Commissioning of a 135 MW Pulsed Power Supply at the Wuhan National High Magnetic Field Centre*, IEEE Trans. Appl. Supercon. **24** (2014), DOI: 10.1109/TASC.2013.2292305.

[2] B. M. Novac, N. D. Hook, R. Smith, *Magnetic flux-compression driven by exploding single-turn coil*, Proc. IEEE International Power Modular and High Voltage Conference (2010) 129–132, DOI: 10.1109/IPMHCV.2010.5958311.

[3] T. Peng, F. Jiang, Q. Q. Sun, Y. Pan, F. Herlach, L. Li, *Concept Design of 100-T Pulsed Magnet at the Wuhan National High Magnetic Field Centre*, IEEE Trans. Appl. Supercon. **26** (2014), DOI: 10.1109/TASC.2015.2523366.

[4] H. Nojiri, T. Takamasu, S. Todo, K. Uchida, T. Haryama, H. A. Katori, T. Goto, M. Miura, *Generation of 500 T fields by electromagnetic flux compression and their application to cyclotron resonance*, Phys. B **201** (1994) 579–583.

[5] B. E. Kane, A. S. Dzurak, G. R. Facer, R. G. Clark, R. P. Starrett, A. Skougarevsky, N. E. Lumpkin, *Measurement instrumentation for electrical transport experiments in extreme pulsed magnetic fields generated by flux compression*, Rev. Sci. Instr. **69** (1997) 3843–3860.

[6] H. C. Siegmann, *Magnetism in the picosecond time scale with electron accelerators*, Europhys. News **31** (2000) 24–25.

[7] C. H. Back, H. C. Siegmann, *Ultrashort magnetic field pulses and elementary process of magnetization reversal*, J. Mag. Mag. Mater. **200** (1999) 774–785.

[8] H. C. Siegmann, E. L. Garwin, C. Y. Prescott, J. Heidmenn, D. Mauri, D. Weller, R. Allenspech, W. Weber, *Magnetism with picosecond field pulses*, J. Mag. Mag. Mater. **151** (1995) L8–L12.

[9] M. Krupa, L. Soby, *Beam intensity measurements in the Large Hardon Collider*, Proceedings of the 20$^{\text{th}}$ International Conference Mixed Design of Integrated Circuits and Systems (2013) 592–597.

[10] P. Baudrenghien, T. Bohl, T. Linnecar, E. Shaposhnikova, J. Tuckmantel, *Nominal longitudinal parameters for the LHC Beam in the CERN SPS*, Proceedings of the Particle Accelerator Conference **5** (2003) 3050–3052, DOI: 10.1109/PAC.2003.1289810.

[11] D. W. Miller, *Online measurements of LHC Beam parameters with the ATLAS High-Level Triger*, Proceedings of the Real Time Conference (2010) 1–6 DOI: 10.1109/RTC.2010.5750367.

[12] D. J. Griffiths, *Introduction to Electrodynamics*, Prentice Hall, Inc. Upper Saddle River, New Jersey (1981) 471.

[13] E. M. Purcell, *Electricity and Magnetism*, Berkeley Physics Course, Vol. 2, McGraw-Hill Book Company, New York (1965) 252.

[14] F. Ruggiero, *Nominal LHC parameters*, www.lhc-data-exchange.web.cern.ch/lhc-data/exchange/rugiero.pdf/ (access: 03.07.2016) 7$^{\text{th}}$ LTC meeting, 28 May (2003).

[15] K. Mackay, M. Bonfim, D. Givord, Fontaine A., *50 T pulsed magnetic fields in microcoil*, J. Appl. Phys. **87** (2000) 1996–2002.

Department of Informatics
Faculty of Physics and Applied Informatics
University of Łódź
149/153 Pomorska Str., PL-90-236 Łódź, Poland
e-mail: bedastan@uni.lodz.pl

Department of Informatics
Faculty of Physics and Applied Informatics
University of Łódź
149/153 Pomorska Str., PL-90-236 Łódź, Poland
e-mail: julian-p@wp.pl

Presented by Leszek Wojtczak at the Session of the Mathematical-Physical Commission of the Łódź Society of Sciences and Arts on November 3, 2016.

POLA MAGNETYCZNE I ELEKTRYCZNE WYTWARZANE PRZEZ PACZKĘ PROTONÓW Z AKCELERATORA LHC I PROJEKT KOMORY DO BADAŃ W TYCH POLACH

S t r e s z c z e n i e

W artykule opisano metodę wyznaczania rozkładu przestrzennego indukcji pola magnetycznego i natężenia pola elektrycznego, które są wytwarzane przez relatywistyczne wiązki cząstek naładowanych. Opisaną metodę zastosowano do wyznaczania rozkładów tych pól w otoczeniu paczki protonów przyspieszanych w LHC. Wykazano, że takie paczki wytwarzają silne impulsowe pola magnetyczne o indukcji od kilkuset do kilkudziesięciu T w obszarze o rozmiarach kilku cm. Pola te mogą być z powodzeniem wykorzystane do badana właściwości materiałów w nowej, dotychczas nie osiągalnej skali przedziałów czasu rzędu fs. Opisane również projekt specjalnej komory, umożliwiającej zdalną wymianę próbek i zbieranie wyników pomiarów prowadzonych w tych polach.

Słowa kluczowe: pole magnetyczne, silny impuls, akcelerator, cząstka, wiązka, zastosowanie